Published by Institute of Physics Publishing for SISSA/ISAS

Received: *August 1, 2003*
Accepted: *August 1, 2003*

Two-loop renormalization for nonanticommutative $N = 1/2$ supersymmetric WZ model

Marcus T. Grisaru

Physics Department, McGill University
Montreal, QC Canada H3A 2T8
E-mail: grisaru@physics.mcgill.ca

Silvia Penati and Alberto Romagnoni

Dipartimento di Fisica dell'Università degli studi di Milano-Bicocca, and
INFN, Sezione di Milano
piazza della Scienza 3, I-20126 Milano, Italy
E-mail: silvia.penati@mib.infn.it, alberto.romagnoni@mib.infn.it

Abstract: We study systematically, through two loops, the divergence structure of the supersymmetric WZ model defined on the $N = 1/2$ nonanticommutative superspace. By introducing a spurion field to represent the supersymmetry breaking term F^3 we are able to perform our calculations using conventional supergraph techniques. Divergent terms proportional to F, F^2 and F^3 are produced (the first two are to be expected on general grounds) but no higher-point divergences are found. By adding *ab initio* F and F^2 terms to the original lagrangian we render the model renormalizable. We determine the renormalization constants and beta functions through two loops, thus making it possible to study the renormalization group flow of the nonanticommutation parameter.

Keywords: Renormalization Regularization and Renormalons, Supersymmetry Breaking, Supersymmetric Effective Theories, Superspaces.

Contents

1. Introduction

In the past few years, the properties of field theories defined over a noncommutative (NC) space-time have been studied extensively, both at the classical and at the quantum level (for a review and references see for instance [1]). More recently, extensions of noncommutative geometry ideas to superspace have been considered [2, 5] and investigations of field theories defined over such superspaces have been initiated, both at the classical level [5], at the quantum level [6, 7] and in connection with matrix models [4, 8, 9]. Although the most general non(anti)commutative (N(A)C) extensions involve both space-time x^a and spinor θ^α coordinates, the simplest case is that of N=1 supersymmetric theories where the only modification, in a suitably defined *euclidean space*, of the ordinary geometry involves the anticommutator $\{\theta^\alpha, \theta^\beta\} = 2C^{\alpha\beta}$ with C a nonzero constant, all the other (anti)commutators keeping their usual values. For this case Seiberg [5] has described extensions of the usual field theories of chiral (scalar multiplet) and real scalar (vector multiplet) superfields, and in refs. [6, 7] some of the quantum properties of the NC Wess-Zumino model have been investigated at low-loop orders.

The effect of θ-nonanticommutativity for the WZ model is very easy to describe; the action, written in terms of ordinary component fields, is the usual WZ component action augmented by a term proportional to F^3, cubic in the auxiliary field (but without a corresponding $\bar{F}^3$). The $N = 1$ supersymmetry is broken down to $N = 1/2$, and some of the remarkable quantum properties of supersymmetric theories such as the standard nonrenormalization theorems are no longer valid. Other features such as the stability of the vacuum energy and the existence of an antichiral ring, are unchanged. This has been demonstrated in the explicit examples worked out in refs. [6, 7] using superspace or component calculations.

In the present work, initiated after Seiberg's paper appeared, we cover some of the same ground but we are concerned primarily with the perturbative renormalizability properties of the model. To two-loop order we show that, although new divergences are generated, the model is renormalizable provided we augment the NC WZ component action by terms proportional to F and F^2.[1] In particular, the NC parameter $C_{\alpha\beta}$ gets renormalized; by computing the corresponding β-function one can follow its RG flow.

We have found it convenient to use a *spurion* field U [10] to generate the supersymmetry breaking term F^3 (and, subsequently, F^2 and F); this allows us to use standard supergraph methods and ordinary D-algebra techniques [11] to perform all our calculations in superspace.

Our paper is organized as follows: in section 2 we review the $N = 1/2$ euclidean NAC superspace [5] and clarify its relation to previous proposals [3]. In section 3 we introduce the model and describe the general approach we follow. In section 4, for the NAC WZ model, we compute the divergent one-loop contributions and show that the model is renormalizable if we add an F^2 term (together with a tadpole F) to the classical lagrangian. Two–loop divergent contributions with the insertion of these new vertices are then computed in section 5 where we show that the theory is renormalizable at that order. In section 6 we discuss the renormalization at two loops and compute the beta functions for the couplings of the theory. The last section is then devoted to some conclusions. Two appendices are added where we discuss in details the degree of divergence for the most general one–loop and two–loop diagrams with an arbitrary number of insertions of the spurion field U (arbitrary power in the NAC parameter). There we show that, at least up to two loops, only diagrams with a *single* insertion of U can be divergent.

2. $N = 1/2$ non(anti)commutative superspace

It has been recently shown [12, 4, 5, 13] that the IIB superstring in the presence of a graviphoton background defines a superspace geometry with nonanticommutative spinorial coordinates.[2]

In [3] the most general structure of non(anti)commutative superspaces was discussed by studying the compatibility conditions between the presence of nontrivial commutation relations for bosonic and/or fermionic variables and the presence of supersymmetry. If we

[1] On general grounds, unless forbidden by some symmetry, such terms may be expected to accompany higher powers such as F^3.

[2] Non-anticommutative structures in field theory and gravity have been studied in different contexts [14].

work in Minkowski signature, imposing the extra condition for the algebra of the coordinates to be associative brings in quite severe constraints which allow, as the only nontrivial commutators, $[x,\theta]$, $[x,\bar\theta]$ and $[x,x]$. However, it was shown in [3] that euclidean signature is less restrictive and a NAC superspace with $\{\theta,\theta\}$ different from zero can be defined consistently with associativity.

Rigorously, a superspace with euclidean signature can be defined only when extended susy is present because of the impossibility of assigning consistent reality conditions for the pair of Weyl fermions θ_α, $\bar\theta_{\dot\alpha}$ (for a detailed review on the subject see for instance [15]). This is the reason why in [3] $N=2$ euclidean NAC superspace was considered. However, in the $N=1$ case one can still define a superspace with euclidean signature by temporarly doubling the fermionic degrees of freedom.[3] In this context it is then clear that the description of $N=1$ euclidean superspace is formally equivalent to euclidean $N=2$.

We briefly review the results of [3]. We describe $N=2$ euclidean superspace by coordinates $(x^{\alpha\dot\alpha},\theta^\alpha,\bar\theta^\alpha,\theta^{\dot\alpha},\bar\theta^{\dot\alpha})$ subject to the complex conjugation conditions

$$\begin{aligned}(\theta^\alpha)^* &= i\bar\theta_\alpha\,; \qquad & (\bar\theta^\alpha)^* &= -i\theta_\alpha \\ (\theta_\alpha)^* &= -i\bar\theta^\alpha\,; \qquad & (\bar\theta_\alpha)^* &= i\theta^\alpha\end{aligned} \tag{2.1}$$

and the same for dot variables. There are no h.c. relations between θ^α and $\theta^{\dot\alpha}$.

In [3] we chose a nonchiral representation for the covariant spinor derivatives and susy charges, but this choice brings us to a NAC algebra where $\{\theta,\theta\}$ different from zero necessarily implies nonvanishing commutators between θ's and x's.

Instead, if we use a chiral representation (we consider only the left sector and use the conventions of [11])

$$\begin{aligned}Q_\alpha &= i(\partial_\alpha - i\theta^{\dot\alpha}\partial_{\alpha\dot\alpha})\,; \qquad & Q_{\dot\alpha} &= i\partial_{\dot\alpha} \\ D_\alpha &= \partial_\alpha\,; & D_{\dot\alpha} &= \partial_{\dot\alpha} + i\theta^\alpha\partial_{\alpha\dot\alpha}\end{aligned} \tag{2.2}$$

the susy transformations of the coordinates are

$$\delta x^{\alpha\dot\alpha} = -i\epsilon^\alpha\theta^{\dot\alpha}\,, \qquad \delta\theta^\alpha = \epsilon^\alpha\,, \qquad \delta\theta^{\dot\alpha} = \epsilon^{\dot\alpha} \tag{2.3}$$

and the NAC algebra

$$\{\theta^\alpha,\theta^\beta\} = 2C^{\alpha\beta} \qquad \text{the rest} = 0 \tag{2.4}$$

with $C^{\alpha\beta} = C^{\beta\alpha}$ constant, is compatible with (2.3) and is associative. According to the general discussion in [3] it is easy to see that the algebra of derivatives gets modified as

$$\begin{aligned}&\{D_\alpha, D_\beta\}_* = 0\,, \qquad \{D_\alpha, D_{\dot\alpha}\}_* = i\partial_{\alpha\dot\alpha} \\ &\{D_{\dot\alpha}, D_{\dot\beta}\}_* = -2C^{\alpha\beta}\partial_{\alpha\dot\alpha}\partial_{\beta\dot\beta}\end{aligned} \tag{2.5}$$

while the algebra of the susy charges is not modified. One might conclude that in this representation susy is not broken. However, the modification of the anticommutation relations between covariant derivatives makes it difficult to proceed and consistently define (anti)chiral representations.

[3] S.P. acknowledges a discussion with N. Seiberg on this point.

In [5] an alternative proposal was made which starts with a different chiral representation for derivatives and charges

$$\begin{aligned} Q_{\dot\alpha} &= i(\partial_{\dot\alpha} - i\theta^\alpha \partial_{\alpha\dot\alpha}) \,, \qquad & Q_\alpha &= i\partial_\alpha \\ D_{\dot\alpha} &= \partial_{\dot\alpha} \,, & D_\alpha &= \partial_\alpha + i\theta^{\dot\alpha}\partial_{\alpha\dot\alpha} \,. \end{aligned} \tag{2.6}$$

In principle the NAC algebra consistent with susy and associativity is of the form

$$\begin{aligned} \{\theta^\alpha, \theta^\beta\} &= 2C^{\alpha\beta} \qquad \{\theta^{\dot\alpha}, \theta^\beta\} = \{\theta^{\dot\alpha}, \theta^{\dot\beta}\} = 0 \\ [x^{\alpha\dot\alpha}, \theta^\beta] &= -2iC^{\alpha\beta}\theta^{\dot\alpha} \\ [x^{\alpha\dot\alpha}, x^{\beta\dot\beta}] &= 2\theta^{\dot\alpha}C^{\alpha\beta}\theta^{\dot\beta} \end{aligned} \tag{2.7}$$

but a suitable change of variable

$$y^{\alpha\dot\alpha} = x^{\alpha\dot\alpha} - i\theta^\alpha\theta^{\dot\alpha} \tag{2.8}$$

avoids dealing with noncommuting x's. Therefore the superspace described in terms of $(y^{\alpha\dot\alpha}, \theta^\alpha, \bar\theta^\alpha, \theta^{\dot\alpha}, \bar\theta^{\dot\alpha})$ is dressed with a nonanticommutative geometry given by (2.4). In this case the algebra of the covariant spinor derivatives is not modified, while

$$\begin{aligned} \{Q_\alpha, Q_\beta\}_* &= 0 \,, \qquad \{Q_\alpha, Q_{\dot\alpha}\}_* = i\partial_{\alpha\dot\alpha} \\ \{Q_{\dot\alpha}, Q_{\dot\beta}\}_* &= 2C^{\alpha\beta}\partial_{\alpha\dot\alpha}\partial_{\beta\dot\beta} \,. \end{aligned} \tag{2.9}$$

Therefore the supersymmetry is explicitly broken [5] on the class of smooth functions defined on this superspace. Supersymmetry seems to be broken in general to $N = 1/2$ [5, 13, 16]. We note that the susy-breaking term is quadratic in the bosonic derivatives, so it does not spoil the previous statement about consistency of (2.4) with supersymmetry invariance of the fundamental algebra of the coordinates.

Following Seiberg we realize the NAC geometry on the smooth superfunctions defined on this superspace by introducing the nonanticommutative (but associative) product

$$\begin{aligned} \phi * \psi &= \phi e^{-\overleftarrow{\partial}_\alpha C^{\alpha\beta} \overrightarrow{\partial}_\beta} \psi \\ &= \phi\psi - \phi \overleftarrow{\partial}_\alpha C^{\alpha\beta} \overrightarrow{\partial}_\beta \psi + \frac{1}{2} \phi \overleftarrow{\partial}_\alpha \overleftarrow{\partial}_\gamma C^{\alpha\beta} C^{\gamma\delta} \overrightarrow{\partial}_\delta \overrightarrow{\partial}_\beta \psi \\ &= \phi\psi - \phi \overleftarrow{\partial}_\alpha C^{\alpha\beta} \overrightarrow{\partial}_\beta \psi - \frac{1}{2} C^2 \partial^2\phi \partial^2\psi \end{aligned} \tag{2.10}$$

where we have defined $C^2 = C^{\alpha\beta}C_{\alpha\beta}$. Since the covariant derivatives (2.6) are still derivations for this product, if we define (anti)chiral superfields as usual the classes of (anti)chirals are still closed.

3. The $N = 1/2$ WZ model: generalities

On the non(anti)commutative superspace described in the previous section we define the WZ model as given by the ordinary cubic action where products of superfields are generalized to the star product (2.10). We study the model at the quantum level by performing its renormalization up to two loops.

JHEP08(2003)003

We consider the classical action

$$S=\int d^8z\bar{\Phi}\Phi-\frac{m}{2}\int d^6z\Phi^2-\frac{\bar{m}}{2}\int d^6\bar{z}\bar{\Phi}^2-\frac{g}{3}\int d^6z\Phi*\Phi*\Phi-\frac{\bar{g}}{3}\int d^6\bar{z}\bar{\Phi}*\bar{\Phi}*\bar{\Phi}\,. \quad (3.1)$$

This action is generically complex since no h.c. relations are assumed for fields, masses and couplings. Performing the expansion of the star product as in (2.10) and neglecting total superspace derivatives, the cubic interaction terms reduce to the usual WZ interactions augmented by the nonsupersymmetric component term $\frac{g}{6}\int d^4xC^2F^3$. The action takes the form [5]

$$S=\int d^8z\bar{\Phi}\Phi-\frac{m}{2}\int d^6z\Phi^2-\frac{\bar{m}}{2}\int d^6\bar{z}\bar{\Phi}^2-\frac{g}{3}\int d^6z\Phi^3-\frac{\bar{g}}{3}\int d^6\bar{z}\bar{\Phi}^3+\frac{g}{6}\int d^8zU(D^2\Phi)^3 \quad (3.2)$$

where we have introduced the external, constant spurion superfield $U=\theta^2\bar{\theta}^2C^2$ in order to deal with a well-defined superspace expression for the extra term proportional to the NC parameter. We note that an equivalent description can be given where the extra term is expressed as $\int d^2\theta\Phi(D^2\Phi)^2$. However, the integrand is not chiral and in principle it is not clear why it should be inserted as an F-term in the action. Our choice allows us to use all the standard tools and techniques of superspace perturbation theory.

The action in components reads ($\Phi|=\phi$, $D_\alpha\Phi|=\psi_\alpha$, $D^2\Phi|=F$ and analogously for the antichiral components)

$$\begin{aligned}S=&\int d^4x\Big[\phi\Box\bar{\phi}+F\bar{F}-GF-\bar{G}\bar{F}+\frac{g}{6}C^2F^3+\psi^\alpha i\partial_\alpha^{\dot{\alpha}}\bar{\psi}_{\dot{\alpha}}-\\&-\frac{m}{2}\psi^\alpha\psi_\alpha-\frac{\bar{m}}{2}\bar{\psi}^{\dot{\alpha}}\bar{\psi}_{\dot{\alpha}}-g\phi\psi^\alpha\psi_\alpha-\bar{g}\bar{\phi}\bar{\psi}^{\dot{\alpha}}\bar{\psi}_{\dot{\alpha}}\Big]\end{aligned} \quad (3.3)$$

where we have defined

$$\begin{aligned}G&=m\phi+g\phi^2\\ \bar{G}&=\bar{m}\bar{\phi}+\bar{g}\bar{\phi}^2\end{aligned} \quad (3.4)$$

The auxilary fields F and $\bar{F}$ satisfy the algebraic equations of motion (EOM)

$$F=\bar{G}\,,\qquad \bar{F}=G-\frac{g}{2}C^2F^2=G-\frac{g}{2}C^2\bar{G}^2\,. \quad (3.5)$$

We perform quantum–background splitting by setting $\Phi\to\Phi+\Phi_q$ and integrating out the quantum fluctuations Φ_q. The expansion produces the ordinary quadratic and cubic vertices in Φ and $\bar{\Phi}$ plus two new extra vertices from the U term. They are drawn in figure 1.

The propagators are [11] (for notational simplicity, from now on we denote Grassmann dot variables as bar variables)

$$\begin{aligned}\langle\Phi\bar{\Phi}\rangle&=\frac{1}{p^2+m\bar{m}}\delta^{(4)}(\theta-\theta')\\ \langle\Phi\Phi\rangle&=-\frac{\bar{m}D^2}{p^2(p^2+m\bar{m})}\delta^{(4)}(\theta-\theta')\\ \langle\bar{\Phi}\bar{\Phi}\rangle&=-\frac{m\bar{D}^2}{p^2(p^2+m\bar{m})}\delta^{(4)}(\theta-\theta')\,.\end{aligned} \quad (3.6)$$

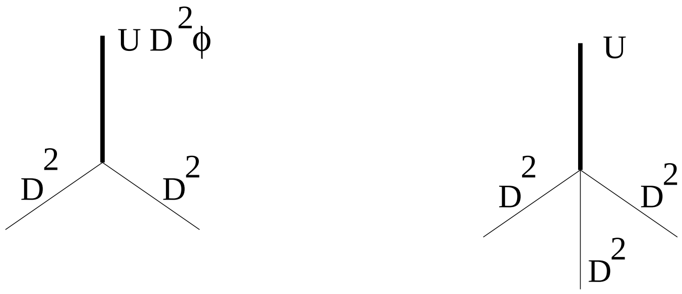

Figure 1: New vertices proportional to the external U superfield.

Moreover, for each chiral (antichiral) field there is an extra $\bar{D}^2$ (D^2) derivative on each line leaving a vertex except for one of the lines at a (anti)chiral vertex.

At a given loop order we draw all supergraph configurations with the corresponding chiral and antichiral derivatives from the vertices and the propagators. Then we perform D-algebra to reduce the supergraph to an ordinary momentum diagram.

We use BPHZ renormalization techniques. Thus, we start with the classical action written in terms of renormalized quantities and order by order perform the subtraction of subdivergences directly on the diagrams. This procedure takes into account automatically the effect of insertion of lower order counterterms.

We work in dimensional regularization ($n = 4 - 2\epsilon$) and minimal subtraction scheme. It is convenient to regularize divergent integrals in the so-called G–scheme

$$\int d^4k f(k) \to G(\epsilon) \int d^n k f(k) \tag{3.7}$$

where $G(\epsilon) = (4\pi)^{-\epsilon}\Gamma(1-\epsilon)$. A practical rule to deal with 4π factors is to neglect them along the calculations and insert a $(4\pi)^2$ for each momentum loop in the final result.

4. One-loop divergences

At one loop we have the ordinary self-energy $\Phi\bar{\Phi}$ diagram which gives a wave function renormalization. The divergent contribution is

$$A_0 \to \frac{2}{\epsilon} g\bar{g} \int d^8 z \Phi\bar{\Phi} \tag{4.1}$$

New divergent diagrams can appear which contain the U-vertices. In appendix A we study the most general one–loop diagram with a given number of Φ, $\bar{\Phi}$ external legs and an arbitrary number of U vertices. We prove that at one loop diagrams with more than one insertion of U vertices are convergent. Moreover, with one U insertion the only divergent topologies are the ones given in figure 2.

Performing D–algebra and keeping only divergent terms all the diagrams give rise to the self-energy momentum integral

$$\int d^4k \frac{1}{(k^2 + m\bar{m})[(p-k)^2 + m\bar{m}]} \to \frac{1}{\epsilon} \,. \tag{4.2}$$

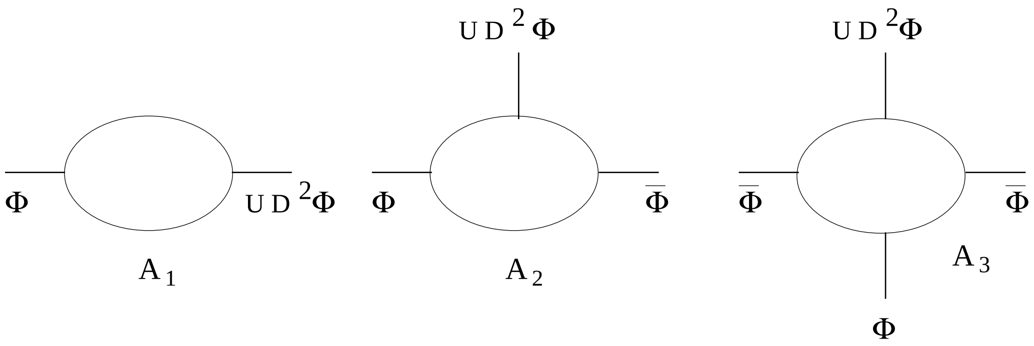

Figure 2: One-loop divergent diagrams with one insertion of the $U(D^2\Phi)^3$-vertex.

Computing the combinatorial factors the divergent contributions are

$$\begin{aligned}
A_1 &\to -\frac{1}{\epsilon}g^2\bar m^2\int d^8z U(D^2\Phi)^2 = -\frac{1}{\epsilon}g^2\bar m^2C^2\int d^4xF^2 \\
A_2 &\to -\frac{4}{\epsilon}g^2\bar g\bar m\int d^8z U(D^2\Phi)^2\bar\Phi = -\frac{4}{\epsilon}g^2\bar g\bar m C^2\int d^4xF^2\bar\phi \\
A_3 &\to -\frac{4}{\epsilon}g^2\bar g^2\int d^8z U(D^2\Phi)^2\bar\Phi^2 = -\frac{4}{\epsilon}g^2\bar g^2C^2\int d^4xF^2\bar\phi^2\,.
\end{aligned} \tag{4.3}$$

In components their sum can be expressed as

$$-\frac{1}{\epsilon}g^2C^2\int d^4x\,\left[\bar m^2\ F^2+4\bar gF^2\bar G\right]. \tag{4.4}$$

We note that, using the classical EOM (3.5) the $\bar G$ in the second term can be replaced by F so that, in superfield form, the divergent contribution takes the form

$$-\frac{1}{\epsilon}g^2\int d^8z\left[\bar m^2U(D^2\Phi)^2+4\bar gU(D^2\Phi)^3\right]. \tag{4.5}$$

The use of the classical EOM can be justified in the following manner: We have started with the classical vertex proportional to F^3 and have produced, at the one-loop level, a divergence which requires a counterterm proportional to $F^2\bar G$. This counterterm, to be added to the classical lagrangian, is to be used now to cancel the one-loop divergence, but also, at a higher-loop level, to remove subdivergences (which, following BPHZ, are removed by hand). However we can show that inserting such a vertex into a diagram is completely equivalent to inserting the vertex F^3. In fact, let us consider the effect of one field factor F from such an insertion as compared to the factor $\bar G=\bar m\bar\phi+\bar g\bar\phi^2$ or, which is more convenient, $F-\bar m\bar\phi$ as compared to $\bar g\bar\phi^2$. We shall need the following component propagators:

$$\begin{aligned}
\langle F\bar F\rangle &= -\frac{\Box}{\Box-m\bar m} \\
\langle\bar\phi\bar F\rangle &= -\frac{m}{\Box-m\bar m} \\
\langle\phi F\rangle &= -\frac{\bar m}{\Box-m\bar m} \\
\langle\phi\bar\phi\rangle &= -\frac{1}{\Box-m\bar m}\,.
\end{aligned} \tag{4.6}$$

JHEP08(2003)003

In the Wick expansion, the operators in $F - \bar{m}\bar{\phi}$ can be contracted either with ϕ in the cubic vertices $-g\phi^2 F$ or $-g\phi\psi^\alpha\psi_\alpha$ but given the form of the propagators the result is zero; or with the $\bar{F}$ in the cubic vertex $-\bar{g}\bar{\phi}^2\bar{F}$ and, given the form of the propagators, the result is $1 \cdot \bar{g}\bar{\phi}^2$ thus establishing that $F - \bar{m}\bar{\phi}$ is completely equivalent to $\bar{g}\bar{\phi}^2$. Higher powers of these operators can be treated in the same manner (except for some combinatorial factors — see section 4) thus showing the equivalence of the two forms of counterterms when inserted into diagrams.

Finally, in comparing *bare* lagrangians, i.e. the renormalized lagrangians plus counterterms, the equivalence of the two sets of counterterms follows just by using the corresponding equations of motion, in particular the equation for $\bar{F}$, that follow from these lagrangians.[4]

4.1 One-loop diagrams with the new term $U(D^2\Phi)^2$

As shown above (see eq. (4.5)), at one loop a divergent term proportional to F^2 appears which is not present in the classical action. This implies that the theory described by (3.1) is not renormalizable. We consider therefore a modified action with the addition of F and F^2 terms, written in superspace with the help of the spurion field U (although the F term could also be written as a perfectly good chiral integral of Φ)

$$\begin{aligned} S = & \int d^8 z \bar{\Phi}\Phi - \frac{m}{2}\int d^6 z \Phi^2 - \frac{\bar{m}}{2}\int d^6 \bar{z} \bar{\Phi}^2 - \frac{g}{3}\int d^6 z \Phi^3 - \frac{\bar{g}}{3}\int d^6 \bar{z} \bar{\Phi}^3 + \\ & + \frac{g}{6}\int d^8 z U (D^2\Phi)^3 + k_1 \bar{m}^4 \int d^8 z U D^2\Phi + k_2 \bar{m}^2 \int d^8 z U (D^2\Phi)^2 \end{aligned} \qquad (4.7)$$

where we have introduced new dimensionless coupling constants k_1 and k_2. This implies the insertion of mass powers. The choice to use $\bar{m}$ rather than m is at this point completly arbitrary but it allows to simplify calculations. The presence of the linear F term is required since linear (divergent) contributions are necessarily produced at the quantum level once a quadratic vertex is present. In principle it (or the F^2 term) could be absorbed by suitable field redefinitions but at the expense of producing other terms; we prefer to keep them explicitly in the classical action.

From the quadratic vertex $U(D^2\Phi)^2$ new topologies of diagrams emerge which give rise to divergent contributions. By using a general procedure like the one described in appendix A we select the new divergent diagrams as given in figure 3. Again, diagrams with more than one U-insertion are convergent.

Computing the combinatorial factors, the contributions are

$$\begin{aligned} \widetilde{A}_1 & \to -\frac{2}{\epsilon}\, k_2\, g\bar{m}^4 \int d^8 z U (D^2\Phi) = -\frac{2}{\epsilon} k_2 g \bar{m}^4 C^2 \int d^4 x F \\ \widetilde{A}_2 & \to -\frac{8}{\epsilon} k_2 g\bar{g}\bar{m}^3 \int d^8 z U (D^2\Phi)\bar{\Phi} = -\frac{8}{\epsilon} k_2 g\bar{g}\bar{m}^3 C^2 \int d^4 x F\bar{\phi} \\ \widetilde{A}_3 & \to -\frac{8}{\epsilon} k_2 g\bar{g}^2\bar{m}^2 \int d^8 z U (D^2\Phi)\bar{\Phi}^2 = -\frac{8}{\epsilon} k_2 g\bar{g}^2\bar{m}^2 C^2 \int d^4 x F\bar{\phi}^2 \end{aligned} \qquad (4.8)$$

[4] We emphasize that the use of the classical EOM is valid only in the limited sense employed here. In general, the full *quantum* equations must be used when dealing with the full effective action.

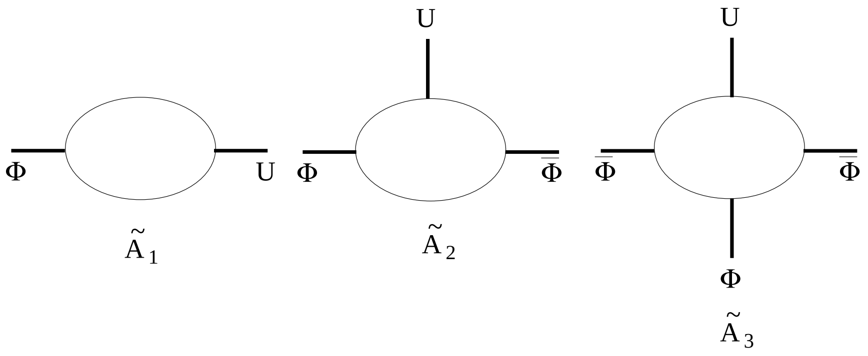

Figure 3: One-loop divergent diagrams with one insertion of the $U(D^2\Phi)^2$-vertex.

and they sum up to the following divergent expression

$$\widetilde{A}_1 + \widetilde{A}_2 + \widetilde{A}_3 = -\frac{2}{\epsilon} k_2 g \bar{m}^2 C^2 \int d^4x \left[\bar{m}^2 F + 4\bar{g} F \bar{G} \right] . \tag{4.9}$$

Using the classical EOM (3.5) for the F-field the second term is an F^2 contribution.

Therefore, summing everything and reinserting (4π) factors, the total one-loop divergence in superspace language is

$$-\frac{1}{\epsilon}\frac{1}{(4\pi)^2} \int d^8z \left[2k_2 g \bar{m}^4 U(D^2\Phi) + \bar{m}^2 (g^2 + 8k_2 g\bar{g}) U(D^2\Phi)^2 + 4g^2\bar{g} U(D^2\Phi)^3 \right] . \tag{4.10}$$

5. Two-loop divergences

At two loops there is the ordinary self-energy $\Phi\bar{\Phi}$ diagram which induces a wave function renormalization. New divergent contributions can arise by U-insertions due to both quadratic $U(D^2\Phi)^2$ and cubic $U(D^2\Phi)^3$ vertices. In appendix B we give a detailed analysis of potentially divergent diagrams and show that even at two loops divergences can arise only when a single U vertex (quadratic or cubic) is present in the diagram. We list them by omitting diagrams which are convergent after subtraction of subdivergences. Once D-algebra is performed, nonvanishing divergent contributions always reduce to the following momentum integrals (corresponding to the two configurations drawn in figure 4)

$$\begin{aligned} I_1 &= \int \frac{d^n k d^n q}{[k^2 + m\bar{m}]\,[(p-k)^2 + m\bar{m}]\,[q^2 + m\bar{m}]\,[(k-q)^2 + m\bar{m}]} \\ I_2 &= \int \frac{d^n k d^n q}{[k^2 + m\bar{m}]\,[(p-k)^2 + m\bar{m}]\,[q^2 + m\bar{m}]\,[(p-q)^2 + m\bar{m}]} . \end{aligned} \tag{5.1}$$

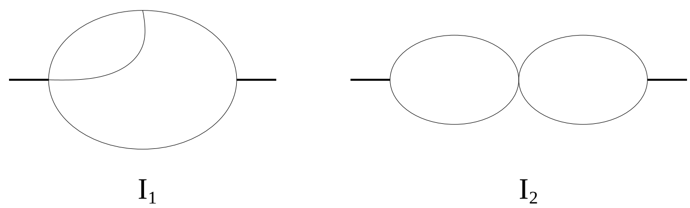

Figure 4: Divergent loop integrals.

In dimensional regularization, after subtraction of the self-energy subdivergences they give

$$I_1 \to -\frac{1}{2\epsilon^2} + \frac{1}{2\epsilon}\,, \qquad I_2 \to -\frac{1}{\epsilon^2}\,. \tag{5.2}$$

The ordinary two-loop contribution to the self-energy $\Phi\bar{\Phi}$ is then

$$-[8I_1]g^2\bar{g}^2 \int d^8z \Phi\bar{\Phi} = -\left[-\frac{1}{\epsilon^2} + \frac{1}{\epsilon}\right] 4g^2\bar{g}^2 \int d^8z \Phi\bar{\Phi}\,. \tag{5.3}$$

We now list all the other divergent contributions classifying them according to the number of external fields. For each configuration we keep distinct the diagrams with a cubic U vertex from the ones with a quadratic one (in the figures they are indicated as tilde quantities).

5.1 One-point functions

At two loops we have the tadpoles drawn in figures 5 and 6.

Computing the combinatorial factors they give

$$\begin{aligned}
T_1:&\ \ [2I_1]g^3\bar{m}^4 \int d^8z U(D^2\Phi) \to \left(-\frac{1}{\epsilon^2} + \frac{1}{\epsilon}\right) g^3\bar{m}^4 C^2 \int d^4x F \\
\widetilde{T}_1:&\ \ [(8+8+16)I_1]k_2 g^2\bar{g}\bar{m}^4 \int d^8z U(D^2\Phi) \to \left(-\frac{1}{\epsilon^2} + \frac{1}{\epsilon}\right) 16k_2 g^2\bar{g}\bar{m}^4 C^2 \int d^4x F\,.
\end{aligned} \tag{5.4}$$

5.2 Two-point functions

The divergent contributions to the two-point functions are given by the graphs in figures 7–10.

Computing the combinatorial factors, we have the following contributions

$$\begin{aligned}
B_1:&\ \ [(4+4+8)I_1 + 4I_2]g^3\bar{g}\bar{m}^2 \int d^8z U(D^2\Phi)^2 \to \left(-\frac{3}{\epsilon^2} + \frac{2}{\epsilon}\right) 4g^3\bar{g}\bar{m}^2 C^2 \int d^4x F^2 \\
\widetilde{B}_1:&\ \ [8I_2]kg^2\bar{g}^2\bar{m}^2 \int d^8z U(D^2\Phi)^2 \to -\frac{8}{\epsilon^2} k_2 g^2\bar{g}^2\bar{m}^2 C^2 \int d^4x\ F^2 \\
B_2:&\ \ [(4+4+8)I_1]g^3\bar{g}\bar{m}^3 \int d^8z U(D^2\Phi)\bar{\Phi} \to \left(-\frac{1}{\epsilon^2} + \frac{1}{\epsilon}\right) 8g^3\bar{g}\bar{m}^3 C^2 \int d^4x F\bar{\phi} \\
\widetilde{B}_2:&\ \ [(16+32+16+16+16+32)I_1]kg^2\bar{g}^2\bar{m}^3 \times \\
&\times \int d^8z U(D^2\Phi)\bar{\Phi} \to \left(-\frac{1}{\epsilon^2} + \frac{1}{\epsilon}\right) 64k_2 g^2\bar{g}^2\bar{m}^3 C^2 \int d^4x\ F\ \bar{\phi}\,.
\end{aligned} \tag{5.5}$$

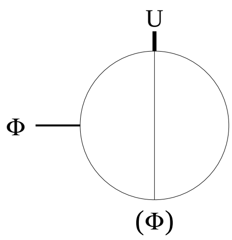

Figure 5: Two-loop contribution $U(D^2\Phi) \quad \to \quad T_1$.

JHEP08(2003)003

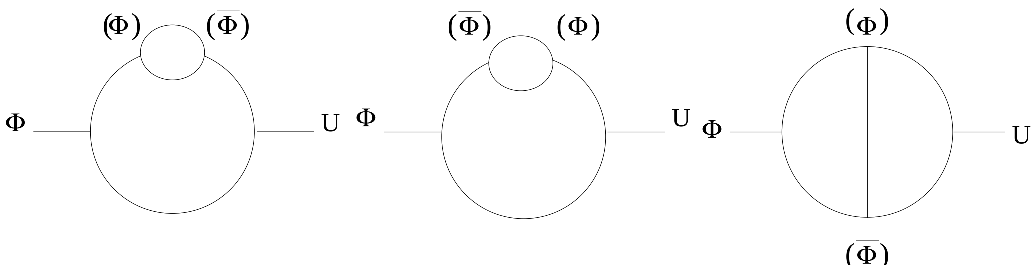

Figure 6: Two-loop contributions $U(D^2\Phi) \quad \to \quad \widetilde{T}_1$.

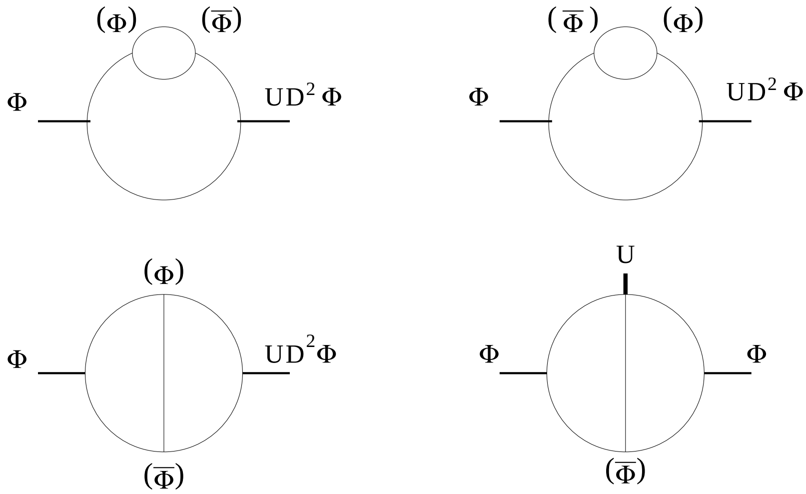

Figure 7: Two-loop contributions $U(D^2\Phi)^2 \quad \to \quad B_1$.

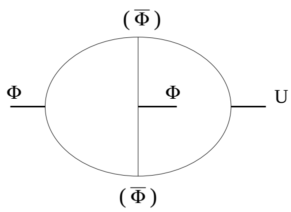

Figure 8: Two-loop contribution $U(D^2\Phi)^2 \quad \to \quad \widetilde{B}_1$.

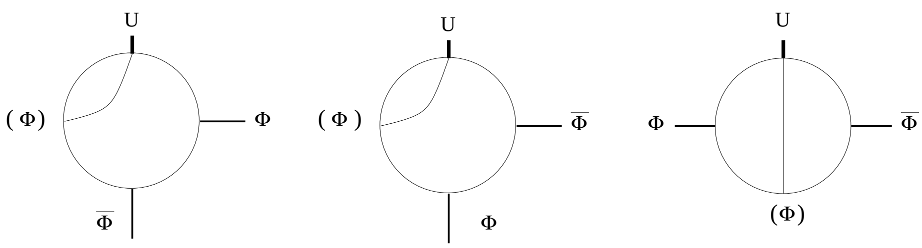

Figure 9: Two-loop contributions $U(D^2\Phi)\bar{\Phi} \quad \to \quad B_2$.

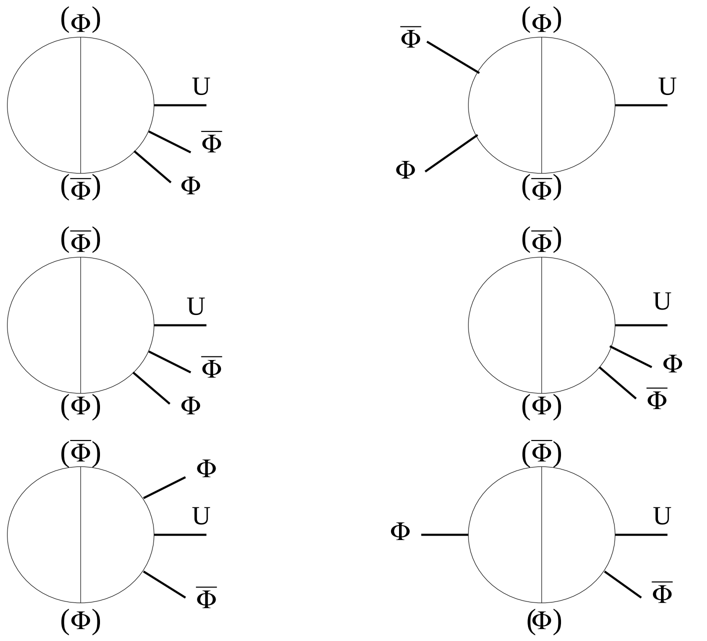

Figure 10: Two-loop contributions $U(D^2\Phi)\bar{\Phi} \quad \rightarrow \quad \widetilde{B}_2$.

5.3 Three-point functions

For the three-point functions the divergent diagrams are drawn in figures 11–14.

Computing the combinatorial factors, we have the contributions

$$
\begin{aligned}
C_1 :&\ \ [4I_2]g^3\bar{g}^2 \int d^8z U(D^2\Phi)^3 \rightarrow -\frac{4}{\epsilon^2} g^3\bar{g}^2 C^2 \int d^4x F^3 \\
C_2 :&\ \ [(8+16+8+8+8+16)I_1 + 16I_2] \times \\
&\times g^3\bar{g}^2\bar{m} \int d^8z U(D^2\Phi)^2\bar{\Phi} \rightarrow \left(-\frac{3}{\epsilon^2}+\frac{2}{\epsilon}\right) 16g^3\bar{g}^2\bar{m}C^2 \int d^4x F^2\bar{\phi} \\
C_3 :&\ \ [(8+8+16+16)I_1]g^3\bar{g}^2\bar{m}^2 \int d^8z U(D^2\Phi)\bar{\Phi}^2 \rightarrow \left(-\frac{1}{\epsilon^2}+\frac{1}{\epsilon}\right) 24g^3\bar{g}^2\bar{m}^2C^2 \int d^4x F\bar{\phi}^2 \\
\widetilde{C}_3 :&\ \ [(32+32+64)I_1]kg^2\bar{g}^3\bar{m}^2 \int d^8z U(D^2\Phi)\bar{\Phi}^2 \rightarrow \left(-\frac{1}{\epsilon^2}+\frac{1}{\epsilon}\right) 64k_2g^2\bar{g}^3\bar{m}^2C^2 \int d^4x F\bar{\phi}^2 .
\end{aligned}
\tag{5.6}
$$

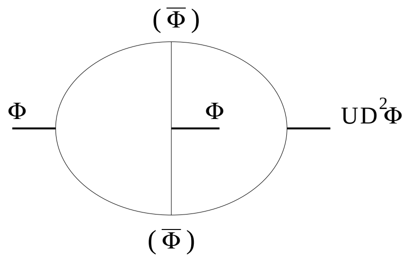

Figure 11: Two-loop contribution $U(D^2\Phi)^3 \quad \rightarrow \quad C_1$.

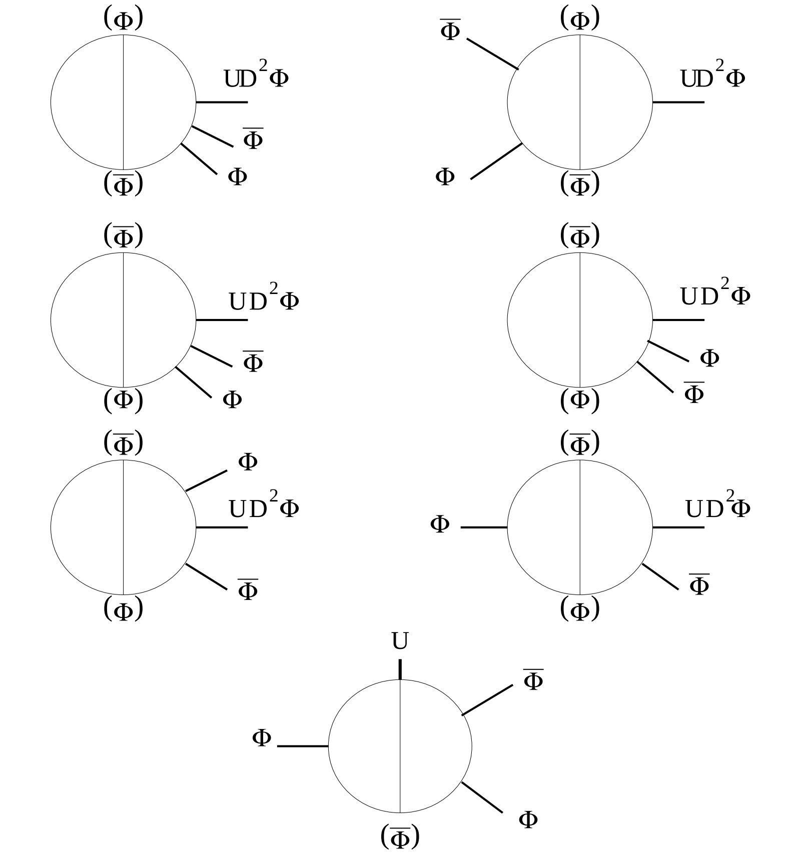

Figure 12: Two-loop contributions $U(D^2\Phi)^2\bar{\Phi} \quad \to \quad C_2$.

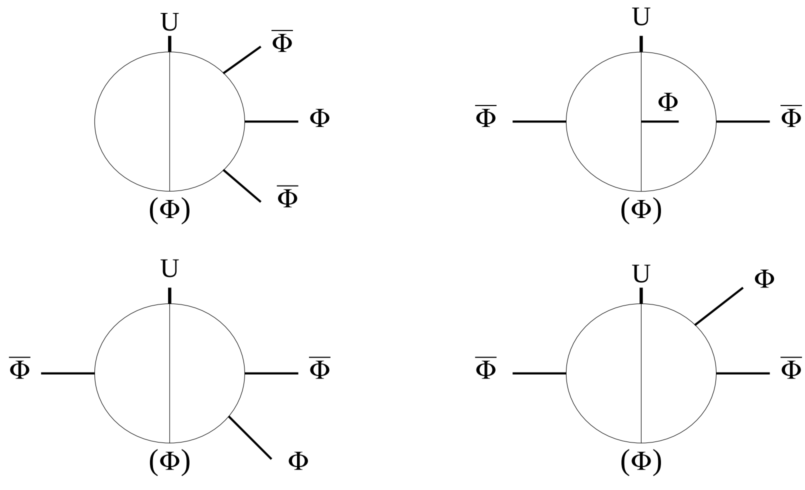

Figure 13: Two-loop contributions $U(D^2\Phi)\bar{\Phi}^2 \quad \to \quad C_3$.

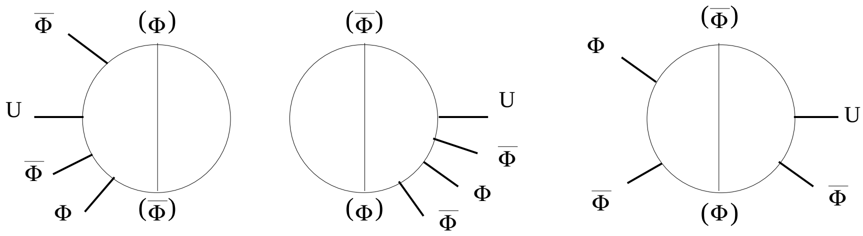

Figure 14: Two-loop contributions $U(D^2\Phi)\bar{\Phi}^2 \quad \rightarrow \quad \widetilde{C}_3$.

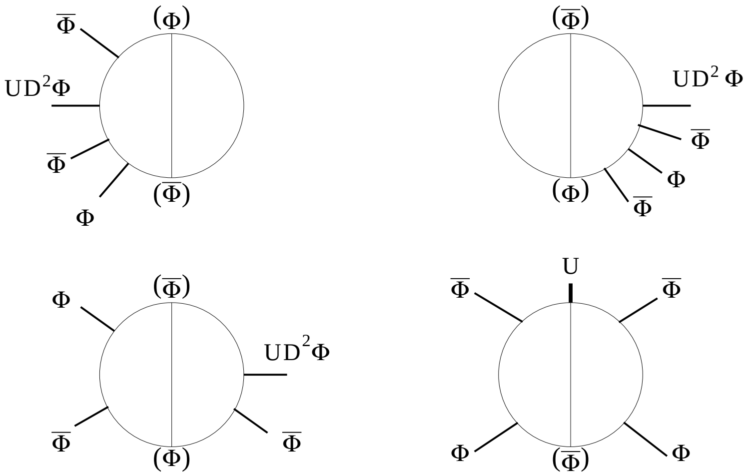

Figure 15: Two-loop contributions $U(D^2\Phi)^2\bar{\Phi}^2 \quad \rightarrow \quad D_1$.

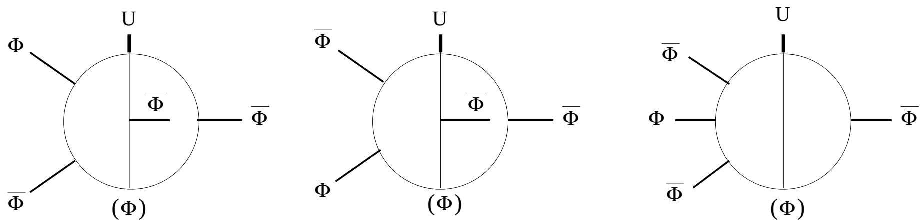

Figure 16: Two-loop contributions $U(D^2\Phi)\bar{\Phi}^3 \quad \rightarrow \quad D_2$.

5.4 Four-point functions

For the 4-point functions the graphs drawn in figures 15, 16 give divergent contributions to the action.

Computing the combinatorial factors, the contributions are

$$\begin{aligned} D_1: \quad & [(16{+}16{+}32)I_1{+}16I_2]g^3\bar{g}^3\int d^8z U(D^2\Phi)^2\bar{\Phi}^2 \rightarrow \left(-\frac{3}{\epsilon^2}+\frac{2}{\epsilon}\right)16g^3\bar{g}^3C^2\int d^4x F^2\bar{\phi}^2 \\ D_2: \quad & [(16{+}16{+}32)I_1] \times \\ & \times g^3\bar{g}^3\bar{m}\int d^8z U(D^2\Phi)\bar{\Phi}^3 \rightarrow \left(-\frac{1}{\epsilon^2}+\frac{1}{\epsilon}\right)32g^3\bar{g}^3\bar{m}C^2\int d^4x F\bar{\phi}^3\,. \end{aligned} \tag{5.7}$$

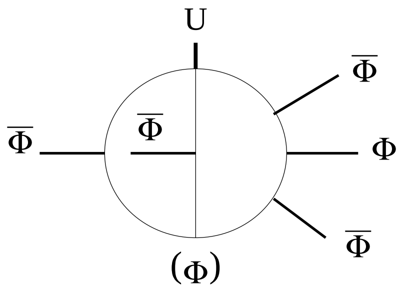

Figure 17: Two-loop contribution $U(D^2\Phi)\bar{\Phi}^4 \quad \rightarrow \quad E_1$.

5.5 Five-point functions

In this case we have only one divergent graph drawn in figure 17.

Computing the combinatorial factors it gives

$$E_1 : [32I_1]g^3\bar{g}^4 \int d^8zU(D^2\Phi)\bar{\Phi}^4 \rightarrow \left(-\frac{1}{\epsilon^2}+\frac{1}{\epsilon}\right) 16g^3\bar{g}^4C^2 \int d^4xF\bar{\phi}^4 \tag{5.8}$$

5.6 Final result

By power counting it is easy to discover that diagrams with more than five external lines are always convergent. Therefore, collecting all the results and inserting back the 4π factors, the total sum of two-loop divergences can be arranged in the following expression

$$g^2\bar{g}C^2 \int d^4x \left[a_1F\bar{G} + a_2F^2\bar{G} + a_3F\bar{G}^2\right] + g^2C^2 \int d^4x \left[a_4F + a_5F^2 + a_6F^3\right] \tag{5.9}$$

where the divergent coefficients are given by

$$\begin{aligned}
a_1 &= \frac{\bar{m}^2}{32\pi^4}(8k_2\bar{g}+g)\left(-\frac{1}{\epsilon^2}+\frac{1}{\epsilon}\right), & a_2 &= \frac{g\bar{g}}{16\pi^4}\left(-\frac{3}{\epsilon^2}+\frac{2}{\epsilon}\right)\\
a_3 &= \frac{g\bar{g}}{16\pi^4}\left(-\frac{1}{\epsilon^2}+\frac{1}{\epsilon}\right), & a_4 &= \frac{\bar{m}^4}{256\pi^4}(g+16k_2\bar{g})\left(-\frac{1}{\epsilon^2}+\frac{1}{\epsilon}\right)\\
a_5 &= \frac{\bar{g}\bar{m}^2}{64\pi^4}\left[\left(-\frac{3}{\epsilon^2}+\frac{2}{\epsilon}\right)g - \frac{2}{\epsilon^2}k_2\bar{g}\right], & a_6 &= -\frac{g\bar{g}^2}{64\pi^4}\frac{1}{\epsilon^2}\,.
\end{aligned} \tag{5.10}$$

Again, as explained in section 2, we can use the classical EOM so as to replace the $\bar{G}$ factors in the first square bracket by factors of F. There is one slight subtlety: as we have seen, replacing F by $(\bar{m}\bar{\phi}+\bar{g}\bar{\phi}^2)$ comes about essentially because one is contracting the former factor with a factor of $\bar{F}$, the contraction being equal to unity. However, if one is contracting two such factors, F^2 with the corresponding factors in $\bar{F}^2$ a combinatorial factor of 2 gets produced. Therefore, the correct replacement is $\bar{G}^2 \rightarrow \frac{1}{2}F^2$.

Summing everything, our final result at two loops, in superspace language, reads

$$\int d^8z \left\{ \frac{\bar{m}^4g^2}{256\pi^4}\left[(g+16k_2\bar{g})\left(-\frac{1}{\epsilon^2}+\frac{1}{\epsilon}\right)\right]U(D^2\Phi) + \right.$$

$$+\frac{\bar{m}^2 g^2}{64\pi^4}\left[g\bar{g}\left(-\frac{5}{\epsilon^2}+\frac{4}{\epsilon}\right)+k_2\bar{g}^2\left(-\frac{18}{\epsilon^2}+\frac{16}{\epsilon}\right)\right]U(D^2\Phi)^2+$$
$$+\frac{g^3\bar{g}^2}{64\pi^4}\left[-\frac{15}{\epsilon^2}+\frac{10}{\epsilon}\right]U(D^2\Phi)^3\Bigg\}. \tag{5.11}$$

6. Renormalization and beta functions

In this section we perform the renormalization of the model at two loops and compute the beta functions for the couplings. In particular, we are interested in the renormalization group equation for the nonanticommutation parameter $C_{\alpha\beta}$. In order to deal with dimensionless quantities, we redefine $C^2 \to \gamma C^2$ with γ the dimensionless coupling subject to renormalization.

In dimensions $n = 4 - 2\epsilon$ we define renormalized quantities as

$$\begin{aligned}
\Phi &= Z_\Phi^{-\frac{1}{2}}\Phi_B\,, & \bar{\Phi} &= Z_{\bar{\Phi}}^{-\frac{1}{2}}\bar{\Phi}_B \\
g &= \mu^{-\epsilon}Z_g^{-1}g_B\,, & \bar{g} &= \mu^{-\epsilon}Z_{\bar{g}}^{-1}\bar{g}_B \\
k_1 &= \mu^{\epsilon}Z_{K_1}^{-1}(k_1)_B\,, & k_2 &= Z_{K_2}^{-1}(k_2)_B \\
\gamma &= Z_\gamma^{-1}\gamma_B
\end{aligned} \tag{6.1}$$

where powers of the renormalization mass μ have been introduced in order to deal with dimensionless renormalized couplings.

From the classical action written in terms of renormalized quantities plus the divergent counterterms we can easily compute the Z functions up to two loops. We can immediately compute Z_g and $Z_{\bar{g}}$ from Z_Φ by requiring that $g\Phi^3$ and $\bar{g}\bar{\Phi}^3$ be not renormalized. If we set set $Z_\Phi = Z_{\bar{\Phi}}$ (in this case there is no h.c. relation which forces this choice) we find

$$\begin{aligned}
gZ_g &= g\left[1+\left(\frac{3}{(4\pi)^2}g\bar{g}-\frac{6}{(4\pi)^4}g^2\bar{g}^2\right)\frac{1}{\epsilon}+\frac{27}{2(4\pi)^4}g^2\bar{g}^2\frac{1}{\epsilon^2}\right] \equiv g+\frac{g_1}{\epsilon}+\frac{g_2}{\epsilon^2} \\
\bar{g}Z_{\bar{g}} &= \bar{g}\left[1+\left(\frac{3}{(4\pi)^2}g\bar{g}-\frac{6}{(4\pi)^4}g^2\bar{g}^2\right)\frac{1}{\epsilon}+\frac{27}{2(4\pi)^4}g^2\bar{g}^2\frac{1}{\epsilon^2}\right] \equiv \bar{g}+\frac{\bar{g}_1}{\epsilon}+\frac{\bar{g}_2}{\epsilon^2}\,.
\end{aligned} \tag{6.2}$$

By writing the counterterms as in eq. (5.11) we also find

$$\gamma\, Z_\gamma \;=\; \gamma\left[1+\left(\frac{24}{(4\pi)^2}g\bar{g}-\frac{240}{(4\pi)^4}g^2\bar{g}^2\right)\frac{1}{\epsilon}+\frac{360}{(4\pi)^4}g^2\bar{g}^2\frac{1}{\epsilon^2}\right] \equiv \gamma+\frac{\gamma_1}{\epsilon}+\frac{\gamma_2}{\epsilon^2}\,. \tag{6.3}$$

From the coefficients of the $1/\epsilon$ pole we can compute the beta functions as

$$\begin{aligned}
\beta_g &= -g\epsilon-\left(1-g\frac{\partial}{\partial g}-\bar{g}\frac{\partial}{\partial\bar{g}}\right)g_1 \\
\beta_{\bar{g}} &= -\bar{g}\epsilon-\left(1-g\frac{\partial}{\partial g}-\bar{g}\frac{\partial}{\partial\bar{g}}\right)\bar{g}_1 \\
\beta_\gamma &= \left(g\frac{\partial}{\partial g}+\bar{g}\frac{\partial}{\partial\bar{g}}\right)\gamma_1
\end{aligned} \tag{6.4}$$

whereas from the poles equations

$$
\begin{aligned}
\left(1-g\frac{\partial}{\partial g}-\bar g\frac{\partial}{\partial \bar g}\right) g_2 &= \frac{\partial g_1}{\partial g}\left(1-g\frac{\partial}{\partial g}-\bar g\frac{\partial}{\partial \bar g}\right) g_1 + \frac{\partial g_1}{\partial \bar g}\left(1-g\frac{\partial}{\partial g}-\bar g\frac{\partial}{\partial \bar g}\right) \bar g_1 \\
\left(1-g\frac{\partial}{\partial g}-\bar g\frac{\partial}{\partial \bar g}\right) \bar g_2 &= \frac{\partial \bar g_1}{\partial g}\left(1-g\frac{\partial}{\partial g}-\bar g\frac{\partial}{\partial \bar g}\right) g_1 + \frac{\partial \bar g_1}{\partial \bar g}\left(1-g\frac{\partial}{\partial g}-\bar g\frac{\partial}{\partial \bar g}\right) \bar g_1 \\
\left(g\frac{\partial}{\partial g}+\bar g\frac{\partial}{\partial \bar g}\right) \gamma_2 &= \frac{\partial \gamma_1}{\partial \gamma}\left(g\frac{\partial}{\partial g}+\bar g\frac{\partial}{\partial \bar g}\right) \gamma_1 - \frac{\partial \gamma_1}{\partial g}\left(1-g\frac{\partial}{\partial g}-\bar g\frac{\partial}{\partial \bar g}\right) g_1 - \\
&\quad -\frac{\partial \gamma_1}{\partial \bar g}\left(1-g\frac{\partial}{\partial g}-\bar g\frac{\partial}{\partial \bar g}\right) \bar g_1
\end{aligned}
\tag{6.5}
$$

we can make a nontrivial check of our calculations.

Inserting the explicit expressions (6.2), (6.3) it is easy to prove that the pole equations are satisfied. Concerning the beta functions, it is evident that the ones for the usual g, $\bar g$ couplings have the standard value

$$
\begin{aligned}
\beta_g &= -\epsilon g + \frac{3}{8\pi^2} g^2 \bar g \left(1 - \frac{g\bar g}{4\pi^2}\right) \\
\beta_{\bar g} &= -\epsilon \bar g + \frac{3}{8\pi^2} g \bar g^2 \left(1 - \frac{g\bar g}{4\pi^2}\right)
\end{aligned}
\tag{6.6}
$$

whereas the beta function for γ is given by

$$
\beta_\gamma = \frac{3}{\pi^2}\gamma g\bar g\left(1 - \frac{5}{4\pi^2} g\bar g\right) . \tag{6.7}
$$

This result is independent of the particular choice $Z_\Phi = Z_{\bar\Phi}$ we have made. However, since we are working in a theory with several coupling constants scheme-dependence may appear already at the two-loop level and undermine the reliability of the second term. Nonetheless, it is interesting to note that a nontrivial fixed point for the C^2 coupling may exist.

7. Conclusions

In this paper we have studied perturbatively the WZ model defined on a nonanticommutative (NAC) superspace where the θ variables are not ordinary Grassmann variables but satisfy a Clifford algebra. Consequently, the usual superspace WZ action is augmented by a term which cannot be written immediately as a superspace integral of superfields. In order to apply standard superspace techniques in the course of our calculations, we have chosen to describe the effects of the NAC (the additional F^3 term in eq. (3.3)) through the introduction of a *spurion* superfield. This is a constant superfield proportional to C^2, the square of the NAC parameter, with only a nonvanishing highest component. We have performed a systematic analysis of all the divergent contributions up to two loops and obtained the following results:

- Up to this order divergent diagrams always contain only one insertion of the spurion. This means that divergent contributions to the effective action proportional to higher powers of C^2 are absent.

JHEP08(2003)003

- At one loop a divergence appears proportional to F^2 in agreement with results found in [6, 7]. In order to deal with a renormalizable model we must start with a classical action containing additional F, F^2 terms (we choose to add also the linear term because from F^2 one naturally starts producing tadpoles). Up to second order in perturbation theory we computed all the divergent diagrams with vertices F^2 and F^3 and showed that no new divergent structures emerge. Up to this order the theory is renormalizable.

- Up to two loops the new divergences which arise due to the F^3 vertex are still logarithmic as in the ordinary, supersymmetric case, thus proving that nonanticommutativity induces a soft-breaking of supersymmetry.

- We have studied the renormalization of the theory and computed the beta functions. Even if at two loops we expect these functions to be affected by scheme dependence it is anyway interesting to see the structure of the beta function associated to the NAC parameter. As appears from our result (6.7) nontrivial fixed points might exist.

The appearance of F^2 divergent terms might lead to the conclusion that the star product gets deformed at the quantum level. On general grounds this shouldn't happen since an alternative way to perform calculations would be to keep the star product implicit and implement in superspace the technologies developed for dealing with NC bosonic coordinates. Indeed, the authors of ref. [9] give a general argument to prove that suitable resummations of this and others terms in the effective potential can be rewritten in terms of star product.

Our results confirm the generalized non-renormalization theorem formulated in [6]. In our language the general structure of the effective action reads

$$\Gamma[\Phi,\bar{\Phi}] = \sum_n \int \prod_{j=1}^{n} d^4x_j \int d^2\theta d^2\bar{\theta} G_n(x_1,\ldots,x_n,U,D^2\bar{D}^2U) F_1(x_1,\theta,\bar{\theta}) \cdots F_n(x_1,\theta,\bar{\theta}) \tag{7.1}$$

where G_n may depend on U linearly and on an arbitrary polynomial in $(D^2\bar{D}^2U)$. Up to two loops the divergent parts of the functions G_n depend only on U and not on its derivatives. It would be interesting to find an argument to prove that this statement remains true at any order in perturbation theory. It would also be interesting to study the model at higher loops and find a general argument for renormalizability at every order.

Finally, we note that our approach can be easily extended to the case of matter coupled to gauge fields.

Acknowledgments

This work has been supported in part by INFN, MURST and the European Commission RTN program HPRN–CT–2000–00131, in which S.P. and A.R. are associated to the University of Padova. The work of M.T.G. is supported by NSF Grant No. PHY-0070475 and by NSERC Grant No. 204540.

JHEP08(2003)003

A. Divergent diagrams from U-insertions

In this appendix we use power counting to prove that at one and two loop order only diagrams with at most one insertion of U vertices can be potentially divergent.

We consider the most general one-loop graph as in figure 18.

This diagram contains p $U(D^2\Phi)^3$ vertices, k $\bar{\Phi}^3$ vertices organized in m groups and $n-k$ vertices Φ^3 distributed among the $\bar{\Phi}$ groups. The total number of external legs is $n+p$ and $k \geq m$. Moreover, we indicate with j_i the number of adjacent $\bar{\Phi}^3$ vertices in the i^{th} group. According to the number of Φ vertices between two $\bar{\Phi}$ blocks the U superfield is inserted between two $\bar{\Phi}$'s, two Φ's or one Φ and one $\bar{\Phi}$.

To study possible divergent configurations we evaluate the mass dimensions of the corresponding integrals once the D-algebra has been performed. The first step is to compute the number of D^2, $\bar{D}^2$ derivatives and the number of propagators initially present in the graph. Then we perform D-algebra and look for the most divergent configurations which are produced. They may occur when we generate momentum factors through the algebraic relations

$$\begin{aligned} D^2\bar{D}^2D^2 &= \Box D^2 \qquad & \bar{D}^2D^2\bar{D}^2 &= \Box\bar{D}^2 \\ [D^\alpha,\bar{D}^2] &= i\partial^{\alpha\dot{\alpha}}\bar{D}_{\dot{\alpha}} \qquad & [\bar{D}^{\dot{\alpha}},D^2] &= i\partial^{\dot{\alpha}\alpha}D_\alpha \end{aligned} \tag{A.1}$$

From the Feynman rules described in the text it is easy to determine that the initial number of D^2 and $\bar{D}^2$ is:

- D^2 derivatives:
  - 2 for every U-vertex
  - 1 for every $\bar{\Phi}$-vertex
  - 1 for every propagator $\langle\Phi\Phi\rangle$

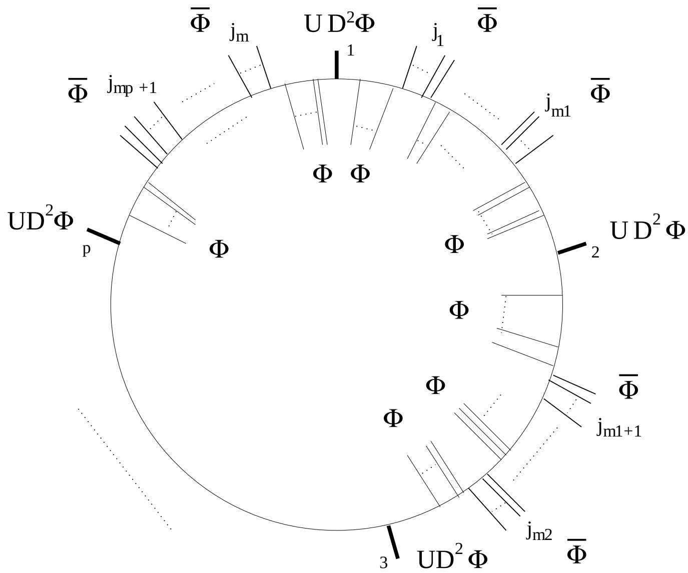

Figure 18.

JHEP08(2003)003

- $\bar{D}^2$ derivatives:
  - 2 for every U-vertex
  - 1 for every Φ-vertex
  - 1 for every propagator $\langle \bar{\Phi}\bar{\Phi} \rangle$
- Propagators:
  - $\langle \bar{\Phi}\bar{\Phi} \rangle$ propagators: $\sum_{i=1}^{m}(j_i - 1) = k - m$
  - $\langle \Phi\bar{\Phi} \rangle$ propagators: $2m$
  - $\langle \Phi\Phi \rangle$ propagators: $(n+p) - (k-m) - 2m$

The total number of derivatives is then

$$D^2 : n - m + 3p$$
$$\bar{D}^2 : n - m + 2p\,.$$

The D-algebra gives a nonzero result when only one pair $D^2\bar{D}^2$ survives inside the loop. We can get rid of additional covariant derivatives by integration by parts at the vertices, either moving derivatives onto external legs or onto internal lines where we can use then the identities (A.1). The most divergent configuration is the one where the maximum number of covariant derivatives remain inside the diagram and combine into momentum factors. We study this case in detail.

We recall that the U superfield has only the $\theta^2\bar{\theta}^2$ component different from zero. This forces us to move one pair $D^2\bar{D}^2$ onto each of $(p-1)$ external U's in order to obtain a final nonvanishing expression, so decreasing the number of D^2 and $\bar{D}^2$ inside the loop by a factor $(p-1)$ (on the remaining U superfield the $d^2\theta d^2\bar{\theta}$ integration will act). Taking into account that if the number of D's inside the loop is different from the number of $\bar{D}$'s the D-algebra gives a vanishing contribution, we have to integrate by parts at least p D^2 derivatives onto external Φ superfields. This implies that at least p external Φ-legs have to be present, i.e.

$$n - k \geqslant p\,. \tag{A.2}$$

Now we can move the remaining derivatives inside the diagram and produce momentum factors as in (A.1).

In conclusion, considering that we have to end up with one pair $D^2\bar{D}^2$ inside the loop, the D-algebra can produce at most a factor

$$\Box^{n-m+p}\,. \tag{A.3}$$

This contribution enters the momentum integrals together with the contributions from the propagators

$\Box^{-2m}$ from the $2m$ $\langle \Phi\bar{\Phi} \rangle$ propagators

$\Box^{-2(n+p-2m)}$ from the $\langle \Phi\Phi \rangle$ and $\langle \bar{\Phi}\bar{\Phi} \rangle$ propagators.

Therefore, the corresponding momentum integral ($\Box \to -q^2$) behaves, in the UV region, as

$$\int d^4q\, \frac{1}{(q^2)^{[n-m+p]}}\,. \tag{A.4}$$

By power counting this integral is divergent if

$$n \leqslant 2 + m - p\,. \tag{A.5}$$

This is consistent with the previous constraints $n \geqslant k + p \geqslant m + p$ if and only if $p \leqslant 1$. This concludes our proof that one-loop diagrams with more than one U-insertion cannot be divergent.

We note that the same conclusion can be easily reached if insertions of the $U(D^2\Phi)^2$ are considered, since the D-algebra is identical.

At this point one can use the same kind of analysis to select the diagrams in figures 2, 3 as the only divergent diagrams from one-loop graphs with one U-insertion.

B. Two-loop divergent diagrams from U-insertions

We now move to two loops and show that again the superficially divergent diagrams can have at most one insertion of the $U(D^2\Phi)^3$ vertex. The procedure is the same as in the one-loop case: we look for the most divergent configurations and we show that, since we have to move factors of $\bar{D}^2$ onto U-fields to get a nonvanishing expression, if there is more than one U-insertion, the momentum factor that we are left with from D-algebra is not sufficient to give a divergent term. Unlike the one-loop case, at this order there are topologically different configurations. Schematically, these are represented in figures 19–24, where it is understood that there are $p \geqslant 1$ insertions of U-terms among k $\bar{\Phi}^3$ vertices organized in m groups $(k \geq m)$ separated by an arbitrary number of Φ^3 vertices whose total number is $(n-k)$.

We analyze the different topologies separately.

Figure 19. In this case, when counting the number of D^2, $\bar{D}^2$ derivatives, we have to take into account that the internal U-vertex brings three D^2 and three $\bar{D}^2$, the internal Φ^3 vertex gives two $\bar{D}^2$. Counting D^2's and $\bar{D}^2$'s from propagators

$$\begin{aligned} \langle\Phi\Phi\rangle\text{propagators} &\to [(n+p+2)-(k-m)-2m]\; D^2 \\ \langle\bar{\Phi}\bar{\Phi}\rangle\text{propagators} &\to (k-m)\bar{D}^2 \end{aligned}$$

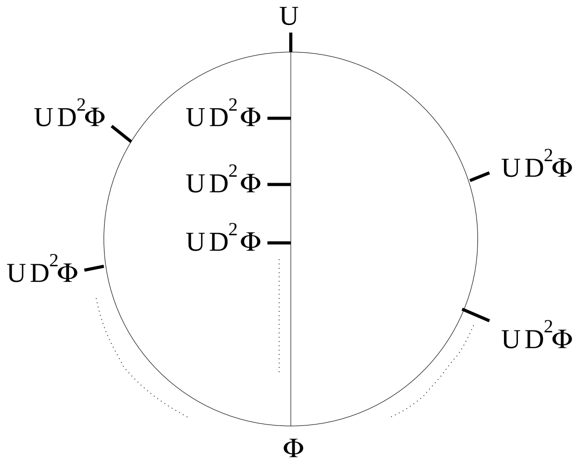

Figure 19.

and from the vertices with external legs, we are led to

$$\begin{aligned} D^2 &: n - m + 3 + 3p \\ \bar{D}^2 &: n - m + 3 + 2p\,. \end{aligned} \tag{B.1}$$

We can proceed exactly as in the one-loop case with the only difference that now the D-algebra ends when two pairs $D^2\bar{D}^2$ remain inside the graph (one for each loop). As before, we need at least p external Φ superfields to get rid of the extra p D^2 derivatives and this imposes the extra constraint

$$n - k \geqslant p\,. \tag{B.2}$$

Finally, from D-algebra at most a momentum factor

$$\Box^{n-m+2+p} \tag{B.3}$$

can be produced. Taking into account the momentum factors from the propagators the most potentially divergent diagram has dimension $8 - 2(n - m + 2 + p)$ and it diverges if

$$n \leqslant 2 + m - p\,. \tag{B.4}$$

Toghether with the other constraint $n \geqslant m + p$ this condition necessarily implies $p \leqslant 1$.

Figure 20. In this case the U-vertex with three internal legs gives three D^2 and three $\bar{D}^2$ and the internal $\bar{\Phi}^3$ vertex gives two D^2. The counting of derivatives from vertices with external legs is the same as in the one-loop case. Moreover, we have a number of derivatives from the chiral and antichiral propagators whose number is

$$\begin{aligned} \langle\Phi\Phi\rangle\text{propagators} &\rightarrow [(n+p+2) - (k-m) - (2m - f + 3))]D^2 \\ \langle\bar{\Phi}\bar{\Phi}\rangle\text{propagators} &\rightarrow (k - m + f)\bar{D}^2 \end{aligned}$$

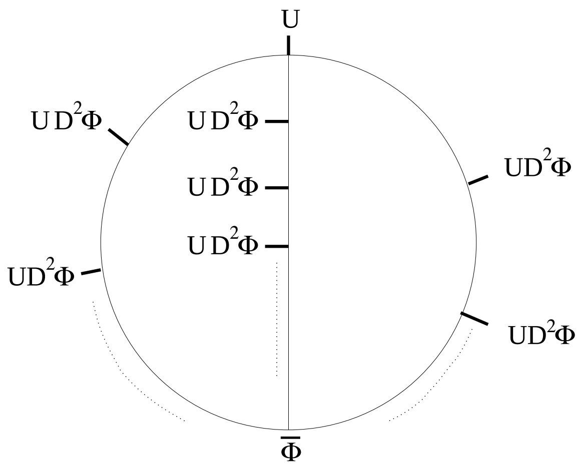

Figure 20.

where $f = 0,1,2,3$ counts the number of $\bar{\Phi}^3$ vertices directly connected to the internal $\bar{\Phi}$ vertex. The total number of covariant derivatives is then

$$\begin{aligned} D^2 &: n - m + 3p + 2 + f \\ \bar{D}^2 &: n - m + 2p + 1 + f \,. \end{aligned} \tag{B.5}$$

In the most divergent configuration, i.e. the one where the maximal number of covariant derivatives remain inside the loop, the D-algebra produces a momentum factor

$$\Box^{n-m+p+f} \tag{B.6}$$

subject to the constraint

$$n \geqslant k + p + 1 \geqslant m + p + 1 \tag{B.7}$$

as follows from the requirement to have at least $(p+1)$ external Φ's to integrate out the additional $(p+1)$ D^2 derivatives.

Since the propagators give a power

$$\Box^{-[2n-2m+2p+2f+1]} \tag{B.8}$$

the dimension of the corresponding integral is $8 - (n - m + f + 1 + p)$. It is then UV divergent if

$$n \leqslant 3 + m - f - p \leqslant 3 + m - p \,. \tag{B.9}$$

Together with $n \geqslant m + p + 1$ it gives $p \leqslant 1$.

Figure 21. This configuration exists only when $p \geqslant 2$. Since the two U-vertices with three internal legs gives six D^2 and six $\bar{D}^2$ and

$$\begin{aligned} \langle \Phi\Phi \rangle \text{propagators} &\to [(n + p + 1) - (k - m) - 2m] D^2 \\ \langle \bar{\Phi}\bar{\Phi} \rangle \text{propagators} &\to (k - m) \bar{D}^2 \end{aligned}$$

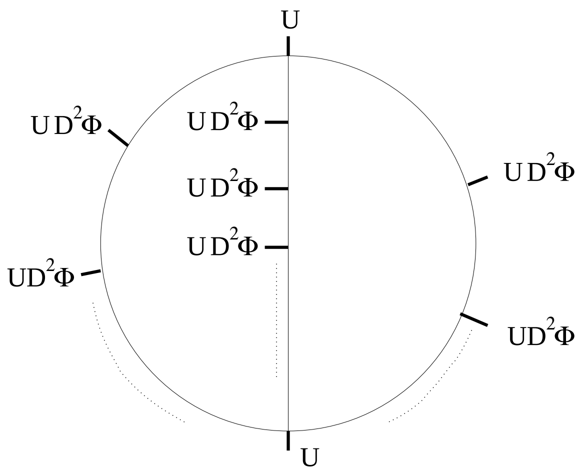

Figure 21.

the total number of covariant derivatives is

$$\begin{aligned} D^2 &: n-m+3p+3 \\ \bar{D}^2 &: n-m+2p+2\,. \end{aligned} \tag{B.10}$$

In the most divergent configuration, the D-algebra produces a momentum factor

$$\Box^{n-m+p+1} \tag{B.11}$$

and the condition

$$n \geqslant k+p+1 \geqslant m+p+1\,. \tag{B.12}$$

Taking into account the factors from the propagators

$$\Box^{-[2n-2m+2p+2]} \tag{B.13}$$

the corresponding momentum integral has dimension $8-(n-m+1+p)$ and diverges if

$$n \leqslant 3+m-p\,. \tag{B.14}$$

Since $n \geqslant m+p+1$, we find $p \leqslant 1$ which is incompatible with the initial assumption $p \geqslant 2$. Therefore, there are no divergent diagrams with this topology.

Figure 22. In this case, since two internal Φ^3 vertices give four $\bar{D}^2$ and

$$\begin{aligned} \langle\Phi\Phi\rangle\text{propagators} &\to [(n+p+3)-(k-m)-2m]D^2 \\ \langle\bar{\Phi}\bar{\Phi}\rangle\text{propagators} &\to (k-m)\bar{D}^2\,, \end{aligned}$$

the total number of covariant derivatives is

$$\begin{aligned} D^2 &: n-m+3+3p \\ \bar{D}^2 &: n-m+4+2p \end{aligned} \tag{B.15}$$

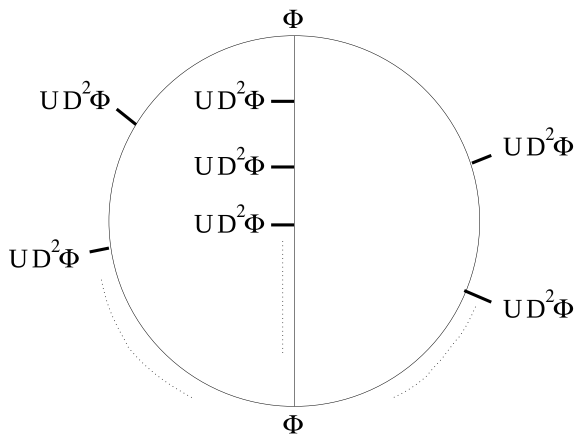

Figure 22.

We first analyze the $p = 1$ case which is the only case with an equal number of D^2 and $\bar{D}^2$ from the beginning. The most convenient way to perform D-algebra is to pull out a D^2 onto the U-vertex by integration by parts. As a consequence, we have to pull out one $\bar{D}^2$ in order to restore the equal number of chiral and antichiral derivatives. In the most divergent configuration, completion of D-algebra produces a momentum factor

$$\Box^{n-m+3}\,. \tag{B.16}$$

The propagators give a factor

$$\Box^{-[2n-2m+8]} \tag{B.17}$$

and the corresponding momentum integral would be divergent if $n \leqslant m-1$ wich is obviously impossible.

In the general case with $p \geqslant 2$, the most divergent configuration is realized when D-algebra produces a momentum factor

$$\Box^{n-m+3+p} \tag{B.18}$$

and the condition

$$n \geqslant m + p - 1 \tag{B.19}$$

is satisfied. Since the propagators give a factor

$$\Box^{-[2n-2m+6+2p]} \tag{B.20}$$

the corresponding momentum integral has dimension $8-2(n-m+3+p)$ and it is divergent if

$$n \leqslant 1 + m - p\,. \tag{B.21}$$

Together with $n \geqslant m+p-1$ it implies $p \leqslant 1$, in contrast with our initial assumption $p \geqslant 2$.

In conclusion we find that the present topology of graphs can never produce UV divergences.

Figure 23. This case can be treated like the figure 20 case by introducing the f parameter which counts the number of $\bar{\Phi}$ vertices directly connected to the internal $\bar{\Phi}^3$. In this case since an internal $\bar{\Phi}^3$ vertex gives two D^2, an internal Φ^3 vertex gives two $\bar{D}^2$,

$$\begin{aligned}
&\langle \Phi\Phi \rangle \text{propagators} \to [(n+p+3) - (k-m) - (2m-f+3))]D^2 \\
&\langle \bar{\Phi}\bar{\Phi} \rangle \text{propagators} \to (k-m+f)\bar{D}^2
\end{aligned}$$

and counting the derivatives from the vertices, the total number of D^2's and $\bar{D}^2$'s is

$$\begin{aligned}
D^2 &: n - m + 3p + 2 + f \\
\bar{D}^2 &: n - m + 2p + 2 + f\,.
\end{aligned} \tag{B.22}$$

In the most divergent configuration, the D-algebra produces a momentum factor

$$\Box^{n-m+p+f+1} \tag{B.23}$$

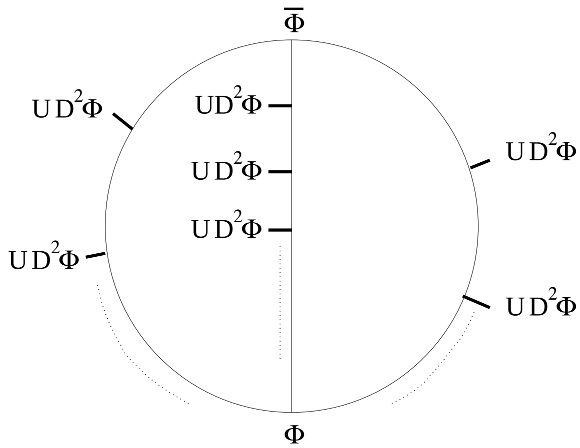

Figure 23.

and the condition

$$n \geqslant k + p \geqslant m + p\,. \tag{B.24}$$

The propagators give a factor

$$\Box^{-[2n-2m+2p+2f+3]} \tag{B.25}$$

so that the corresponding momentum integral has dimension $8 - 2(n - m + f + 2 + p)$ and it is divergent if

$$n \leqslant 2 + m - f - p \leqslant 2 + m - p\,. \tag{B.26}$$

Since $n \geqslant m + p$ a divergence is present when $p \leqslant 1$.

Figure 24. In this case we need introduce the parameter $f' = 0, \ldots, 6$ to count the number of different configurations of external $\bar{\Phi}$ legs directly connected to the internal $\bar{\Phi}^3$ vertices and the configuration where the two internal $\bar{\Phi}^3$ vertices are directly connected.

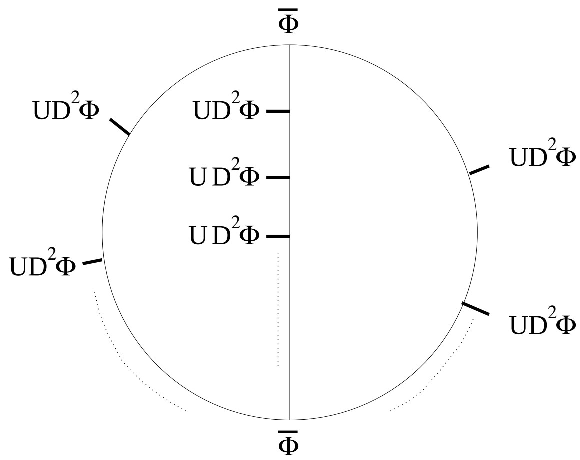

Figure 24.

Since the number of propagators is

$$\langle\Phi\Phi\rangle \text{ propagators: } [(n+p+3)-(k-m)-(2m-f'+6))]$$
$$\langle\bar\Phi\bar\Phi\rangle \text{ propagators: } (k-m+f')$$

the total number of covariant derivatives turns out to be

$$\begin{aligned} &D^2 : n-m+3p+1+f' \\ &\bar D^2 : n-m+2p+f'\,. \end{aligned} \tag{B.27}$$

The most divergent configuration corresponds to the case where a momentum factor

$$\Box^{n-m+p-1+f'} \tag{B.28}$$

is produced by D-algebra, consistent with the condition

$$n \geqslant k+p+1 \geqslant m+p+1\,. \tag{B.29}$$

The propagators give a factor

$$\Box^{-[2n-2m+2p+2f']} \tag{B.30}$$

and the momentum integral has dimension $8-2(n-m+f'+1+p)$. It is divergent when

$$n \leqslant 3+m-f'-p \leqslant 3+m-p\,. \tag{B.31}$$

Since $n \geqslant m+p+1$, we obtain the condition $p \leqslant 1$.

In conclusion, figure 21 and figure 22 configurations never contribute to divergences, whereas the rest can produce divergent terms only when a single insertion of the cubic U vertex is present.

As in the one-loop case, we can make an analogous analysis when considering the insertions of $U(D^2\Phi)^2$ vertices. Since the D-algebra is identical we reach the conclusion that at two loops only diagrams with one U-insertion (both quadratic or cubic) can be divergent. One can now proceed along the same lines to determine which are the actual divergent diagrams for each topology. Precisely, for a given configuration of internal and U vertices, one can determine the number and the distribution of external Φ and/or $\bar\Phi$ legs associated with divergent graphs. As a result one discovers that there cannot be more that five external legs and the diagrams drawn in figures 5–17 exhaust the complete set of two-loop divergent diagrams.

References

[1] R.J. Szabo, *Quantum field theory on noncommutative spaces*, *Phys. Rept.* **378** (2003) 207 [`hep-th/0109162`].

[2] S. Ferrara and M.A. Lledo, *Some aspects of deformations of supersymmetric field theories*, *J. High Energy Phys.* **05** (2000) 008 [`hep-th/0002084`];
S. Ferrara, M.A. Lledo and O. Macia, *Supersymmetry in noncommutative superspaces*, `hep-th/0307039`.

[3] D. Klemm, S. Penati and L. Tamassia, *Non(anti)commutative superspace*, *Class. and Quant. Grav.* **20** (2003) 2905 [hep-th/0104190].

[4] H. Ooguri and C. Vafa, *The C-deformation of gluino and non-planar diagrams*, hep-th/0302109; *Gravity induced C-deformation*, hep-th/0303063.

[5] N. Seiberg, *Noncommutative superspace, $N = 1/2$ supersymmetry, field theory and string theory*, *J. High Energy Phys.* **06** (2003) 010 [hep-th/0305248].

[6] R. Britto, B. Feng and S.-J. Rey, *Deformed superspace, $N = 1/2$ supersymmetry and (non)renormalization theorems*, *J. High Energy Phys.* **07** (2003) 067 [hep-th/0306215].

[7] S. Terashima and J.-T. Yee, *Comments on noncommutative superspace*, hep-th/0306237.

[8] J.-H. Park, *Superfield theories and dual supermatrix models*, hep-th/0307060.

[9] R. Britto, B. Feng and S.-J. Rey, *Non(anti)commutative superspace, UV/IR mixing and open Wilson lines*, *J. High Energy Phys.* **08** (2003) 001 [hep-th/0307091].

[10] L. Girardello and M.T. Grisaru, *Soft breaking of supersymmetry*, *Nucl. Phys.* **B 194** (1982) 65.

[11] S.J. Gates, M.T. Grisaru, M. Roček and W. Siegel, *Superspace*, Benjamin Cummings, Reading 1983 [hep-th/0108200].

[12] J. de Boer, P.A. Grassi and P. van Nieuwenhuizen, *Non-commutative superspace from string theory*, hep-th/0302078.

[13] N. Berkovits and N. Seiberg, *Superstrings in graviphoton background and $N = 1/2 + 3/2$ supersymmetry*, *J. High Energy Phys.* **07** (2003) 010 [hep-th/0306226].

[14] J.H. Schwarz and P. Van Nieuwenhuizen, *Speculations concerning a fermionic substructure of space-time*, *Lett. Nuovo Cim.* **34** (1982) 21;
P. Bouwknegt, J.G. McCarthy and P. van Nieuwenhuizen, *Fusing the coordinates of quantum superspace*, *Phys. Lett.* **B 394** (1997) 82 [hep-th/9611067];
P. Kosinski, J. Lukierski, P. Maslanka and J. Sobczyk, *Quantum deformation of the Poincaré supergroup and kappa deformed superspace*, *J. Phys.* **A 27** (1994) 6827 [hep-th/9405076]; *Quantum deformations of space-time SUSY and noncommutative superfield theory*, hep-th/0011053;
J.W. Moffat, *Non-anticommutative quantum gravity*, hep-th/0011259.

[15] A. Van Proeyen, *Tools for supersymmetry*, hep-th/9910030.

[16] T. Araki, K. Ito and A. Ohtsuka, *Supersymmetric gauge theories on noncommutative superspace*, hep-th/0307076.